https://doi.org/10.46813/2023-144-015

EFFECT OF GRAIN BOUNDARY ON THE CAVITY FORMATION BEHAVIOR IN 1.4 MeV Ar^+ IRRADIATED 18Cr10NiTi-ODS STEEL

G.D. Tolstolutskaya, S.A. Karpov, A.S. Kalchenko, M.A. Tikhonovsky
National Science Center "Kharkov Institute of Physics and Technology", Kharkiv, Ukraine
E-mail: g.d.t@kipt.kharkov.ua

The formation of cavity denuded zones (DZ) near grain boundary (GB) in 18Cr10NiTi-ODS steel with the addition of Y_2O_3-ZrO_2 nano-oxides irradiated with energetic Ar-ions in the dose range of 40…110 displacements per atom (dpa) with simultaneously implanted argon to the levels of 0.08…7 at.% at temperatures of 550…650 ºC was investigated. Transmission electron microscopy has been used to study the microstructure evolution and width of cavity-denuded zones. Denuded zones are found to be dependent of the irradiation conditions, such as irradiation dose, dose rate and temperature. The impact of grain refinement and nanosized oxide precipitates on the characteristics of DZ are examined.

PACS: 61.80.-X, 81.40.CD

INTRODUCTION

Various approaches are being explored to improve the irradiation tolerance of metals, including the introduction of high densities of grain boundaries (GBs), interphase boundaries, or free surfaces. [1, 2]. These boundaries act as sinks for point defects, making them efficient in enhancing the material's resistance to irradiation. Recent studies suggest that nanocrystalline metals with a large specific area of grain boundaries exhibit better irradiation resistance compared to their coarse-grained equivalents, thereby offering a promising way for enhancing the irradiation resistance of many materials [3].

Radiation swelling remains a significant issue for nuclear reactor core parts, along with other radiation-related concerns such as transmutation doping of materials with inert gas atoms (such as helium) that cause degradation of the mechanical properties of reactor materials through high-temperature embrittlement, fatigue, creep, and gas swelling.

Noble gas atoms in solids typically have a tendency to form bonds with vacancy-type defects. This prevents the vacancies created by neutron irradiation from recombining with self-interstitial atoms, causing them to accumulate and form complexes with gas atoms. Interactions between helium-vacancy complexes and thermal vacancies lead to the development of gas porosity (GP) in structural materials at high operating temperatures. During their growth, gas bubbles tend to accumulate at grain boundaries, leading to severe deterioration of materials [4]. On the other hand, both gas bubbles and pores can also contribute to the formation of denuded zones (DZ) near GB, interphase boundaries, or free surfaces. The formation of a DZ can be used to understand how inert gases affect the sink-defect absorption efficiency of different types of boundaries.

To study the effects of high levels of helium and displacement damage, dual ion beam irradiations are often used [5]. Alternative approach is to use heavier noble gases with a larger atomic mass than helium, such as high-energy argon ions, which can effectively create high-level displacement damage and simulate helium effects since the behavior of Ar atoms is thought to be similar to that of He in irradiated metals [6, 7].

The 18Cr10NiTi-ODS steel was found to have the considerable swelling resistance under Ar^+ irradiation [8]. The presence of fine-grained structures with high boundary area and finely distributed dispersoids in this steel enhance the stability of the grain structure and provide defect trapping and annihilation sites, resulting in improved irradiation resistance upon Ar^+ irradiation.

The purpose of this study is to reveal the features of cavity DZ formation during 1.4 MeV Ar irradiation of 18Cr10NiTi-ODS steel with added Y_2O_3-ZrO_2 nano-oxides in terms of the influence of inert gas, grain refinement, nanosized oxide precipitates and irradiation conditions, such as irradiation dose, dose rate and temperature.

1. MATERIAL AND METHODS

The ODS steel used in this study is an austenitic stain – less steel strengthened by Y_2O_3-ZrO_2 nano-oxides which was previously fabricated in NSC KIPT. A detailed technological procedure of production is described in [9]. Grain structure of ODS steel (Fig. 1) was approximately the same for all samples, the average grain size was 1.2…2.0 μm.

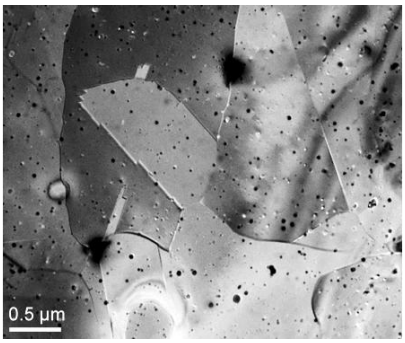

Fig. 1. Pre-irradiation microstructure of 18Cr10NiTi-ODS steel

Significant concentration of precipitates and its near-uniform distribution are observed for all samples. Precipitations size varied from several to hundreds of nanometers, but the last were a few orders less, thus, its contribution to concentration and average size was negligible. The average size of nano-precipitates is estimated at ~ 10 nm and their average density is ~ $7.3 \cdot 10^{21}$ m^{-3}.

The accelerating-measuring system "ESU-2" with a residual target-chamber pressure of ~ $5 \cdot 10^{-5}$ Pa was used for the creation of radiation damage [10]. The argon ions with energy of 1.4 MeV were chosen for irradiation experiments. The irradiation temperature varied from 550 to 650 ºC. The error in the temperature measurement did not exceed ± 5%. The error in the beam current and, consequently of the damage dose, did not exceed ± 10%.

Calculated by SRIM 2008 [11] depth distribution profiles of damage and concentration of Ar atoms implanted in 18Cr10NiTi steel to a dose of $1 \cdot 10^{17}$ cm^{-2} are shown in Fig. 2. The damage calculations are based on the Kinchin-Pease model (KP), with a displacement energy for each alloying elements was set to 40 eV, as recommended in ASTM E521-96 (2009) [12].

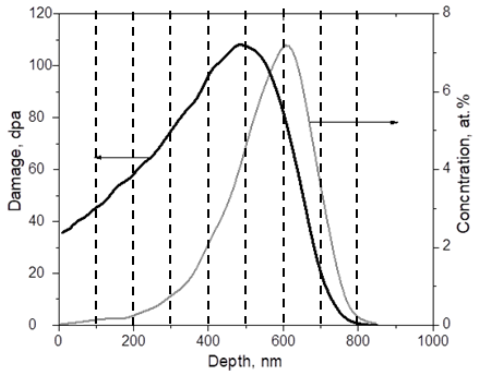

Fig. 2. The depth distribution of damage and Ar atoms concentration calculated with SRIM for 18Cr10NiTi steel irradiated with 1.4 MeV Ar ions to a dose of $1 \cdot 10^{17}$ cm^{-2}

The changes of microstructure as a function of depth are obtained in 100 nm sections from 0 to 800 nm (see Fig. 2). The removing of ~ 100 nm depth-layer of material was performed by the electro-pulse technique.

Microstructural and cavity-denuded zone data were extracted using conventional techniques conducted on JEM-100CX and JEM-2100 transmission electron microscopes, employing standard bright-field techniques.

2. RESULTS AND DISCUSSION

In a previous study, we examined the effects of 1.4 MeV Ar^+ irradiation on the microstructure evolution and swelling behavior of austenitic steel 18Cr10NiTi at temperatures ranging from 550 to 700 ºC [6]. The doses used in the study ranged from 40 to 105 dpa, while the levels of simultaneously implanted argon were between 0.08 and 6.3 at.%. Our findings demonstrated that the microstructure changes induced by irradiation were highly dependent on Ar concentration, implantation temperature and level of displacements per atom.

The present study is focused on the relationship between the development of DZ and the damage dose and implanted argon concentration. Fig. 3 shows that a large number of round-shaped cavities (no obvious facets) with sizes of 1…8 nm was formed after irradiation at 625 ºC, which is the temperature of maximum swelling for this steel under Ar^+ irradiation [6]. It can be seen that the cavity size distribution correlates with the calculated profiles in Fig. 2: the higher dose and concentration of argon, the larger the cavities.

Although a large number of cavities were produced at depth 0…100 nm, there is no obvious formation of DZs around GBs, nor did we observe any defect-denuded zones at GBs at depth 100…200 nm even though the damage and concentration of argon have increased.

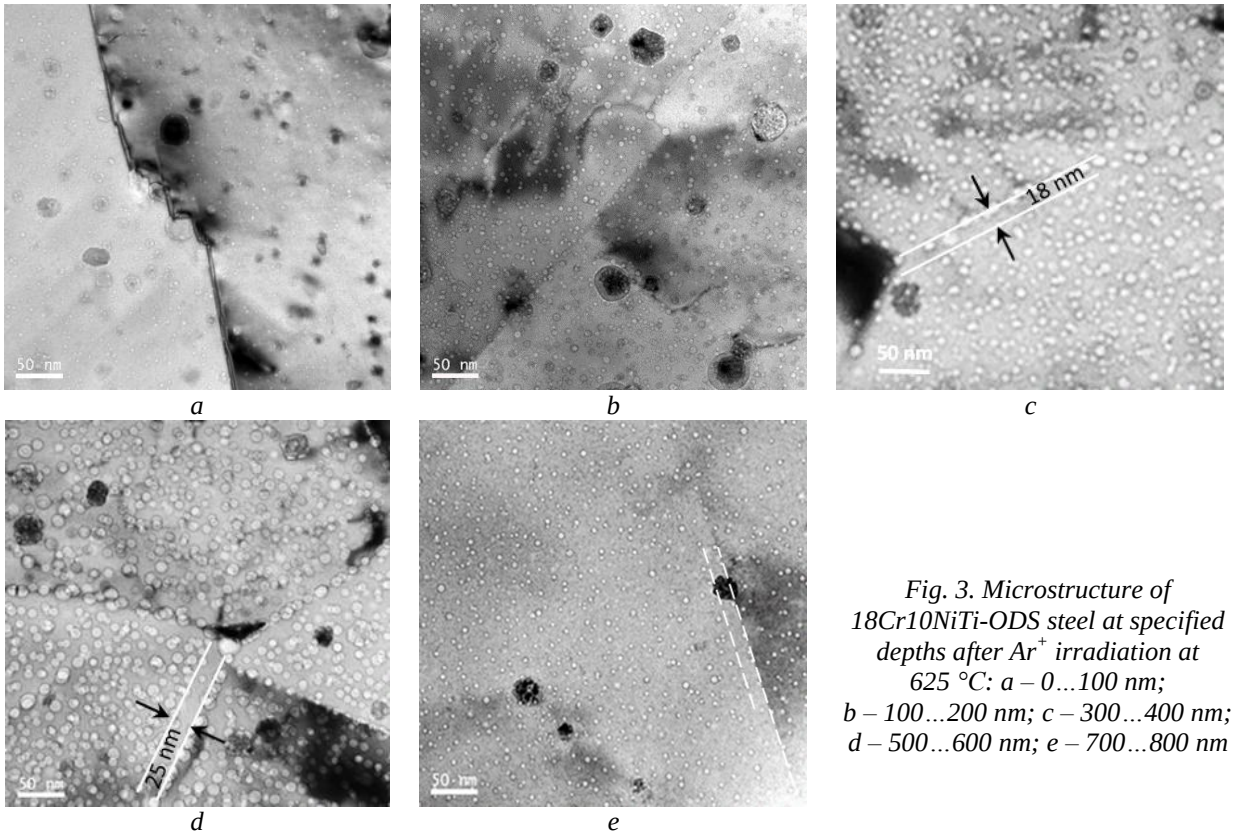

Fig. 3. Microstructure of 18Cr10NiTi-ODS steel at specified depths after Ar^+ irradiation at 625 °C: a – 0…100 nm; b – 100…200 nm; c – 300…400 nm; d – 500…600 nm; e – 700…800 nm

Denudation of grain boundaries is most clearly observed at depths starting at 200 nm, where the argon concentration exceeds 0.4 at.% and the damage dose exceeds 50 dpa. The observed trend agrees well (correlates) with the evolution of cavity diameter, density and swelling with depth in 18Cr10NiTi-ODS steel irradiated with argon ions at the equivalent doses. Cavity size and swelling increase with depth up to the dpa peak region (400…500 nm depth) and then decrease beyond the Ar implantation peak region [13, 14]. It is noteworthy that in almost all cases the cavity size was larger at the GBs than in the grain interiors.

To quantify the width of the DZ, we draw a line along the GB and move it perpendicular to the GB plane towards the grain interior until it intersected with a visible bubble. The distance between the GB and this line was considered as the DZ width (see Fig 3). The measured DZ width was found to be in the range of ~ 17…25 nm for the entire interval of damage and the dose rate at the temperature of 625 ºC.

A systematic and detailed study of the cavity (including voids and bubbles, which are under-pressurized cavities and over-pressurized cavities with gas atoms, respectively) DZ near free surfaces and grain boundaries in neutron- and ion-irradiated simple metals (Cu, Ni, and Fe-Cr) was reported in [15]. It was shown that the cavity DZ width, although gradually decreasing with increasing depth (increasing dose rate), starts from ~ 700 nm. The DZ width values obtained in the current study are much smaller. According to [15, 16], the discrepancy observed can be explained by the dose rate of irradiation, which influences the steady-state concentration of vacancies. When the dose rate is higher, the steady-state concentration of vacancies increases, causing an increase in the concentration gradient of vacancies for a given GB. As a result, a region where the vacancy concentration is insufficient for cavity formation will shift toward the GB, resulting in a narrower DZ. The irradiation dose rate using 1.4 MeV Ar^+ ions was approximately 10^{-2} dpa/s, which was significantly higher than the $1.4 \cdot 10^{-3}$ dpa/s used in reference [15]. This higher dose rate may lead to a smaller DZ. In addition, when helium is introduced through neutron transmutation or co-injection, DZ with narrower widths than those of voids were observed. This is probably due to the formation of He-vacancy complexes, which have higher migration energy and therefore result in a smaller cavity denuded zone width. A similar trend can be seen in the case of argon irradiation.

The formation of DZs is influenced by various factors, such as the steady-state vacancy concentration, diffusion temperature, and duration, as it is a diffusion-controlled process [17]. Fig. 4 shows the effect of irradiation temperature on microstructure of 18Cr10NiTi-ODS steel at depths 500…600 nm and cavities denuded zone in the vicinity of grain boundaries the after 1.4 MeV Ar^+ irradiation at 570…645 °C.

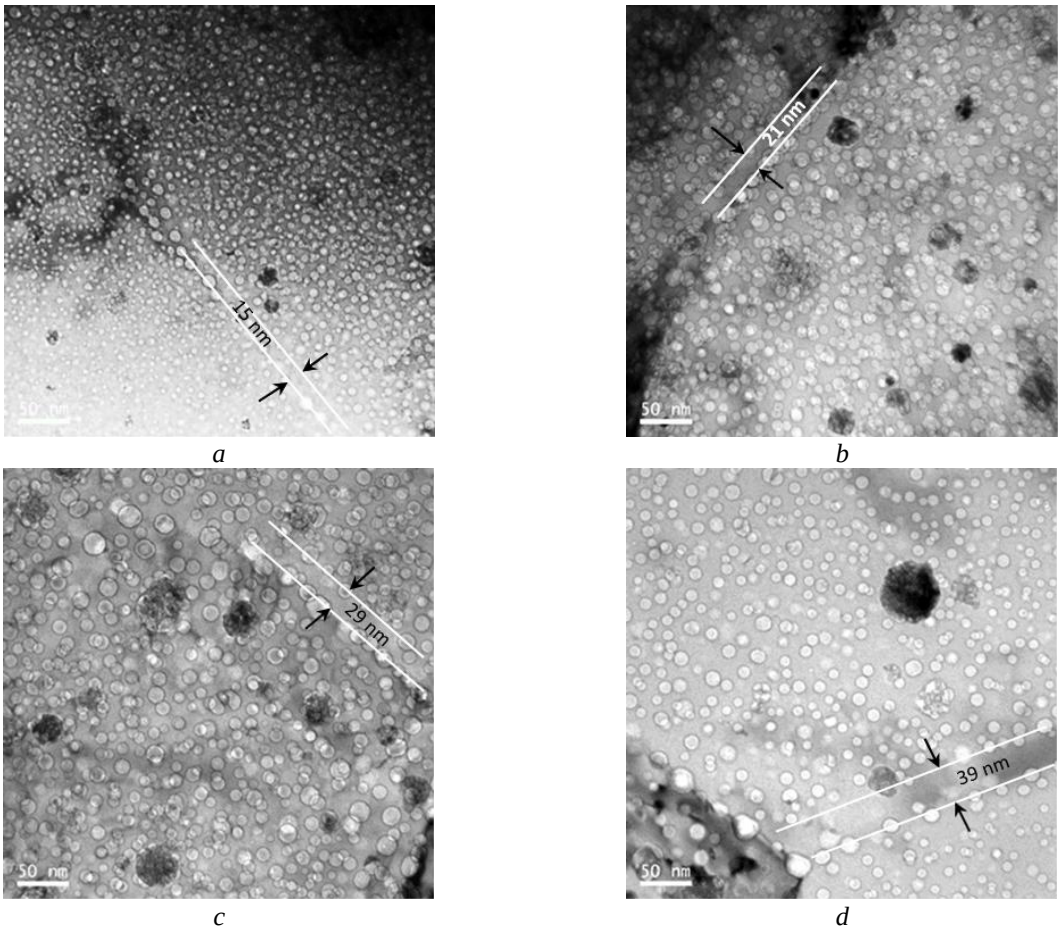

Fig. 4. Microstructure of 18Cr10NiTi-ODS steel at depths 500…600 nm after Ar^+ irradiation at 570 (a), 585 (b), 600 (c), and 645 °C (d)

In the present study, DZs were observed when Ar ion irradiation was performed at temperatures above 570 °C. The measured DZ width was ~ 15…9 nm and increased with increasing irradiation temperature, indicating the influence of temperature. For a lower irradiation temperature, the diffusivity of vacancies is smaller, resulting in higher vacancy supersaturations and hence smaller DZ widths. As temperature increases, diffusivity of vacancies increases while supersaturation decreases and the cavities DZ width increased from 15 to 39 nm at 570 and 645 °C, respectively.

While extensive research has been conducted on the impact of GP in metals, and general patterns of GP development based on damage rate, dose, and irradiation temperature have been published [18, 19], it is worth noting that each structural material exhibits its own specific patterns.

The development of GP and the formation of DZ has a more complicated character in 18Cr10NiTi-ODS steel with its increased GB population and nano-sized oxide precipitates compared to conventional 18Cr10NiTi steel [8] (Fig. 5).

The numbers in Fig. 5 indicate the formation of larger bubbles along the grain boundaries (1) and/or dislocations (2). The formation of DZ near grain boundaries (3) and no denuded grain boundaries was observed (4). The heterogeneous distribution of bubbles in size and density (5), the interaction of bubbles with precipitates (6) the array of parallel chains of bubbles (7) are also indicated.

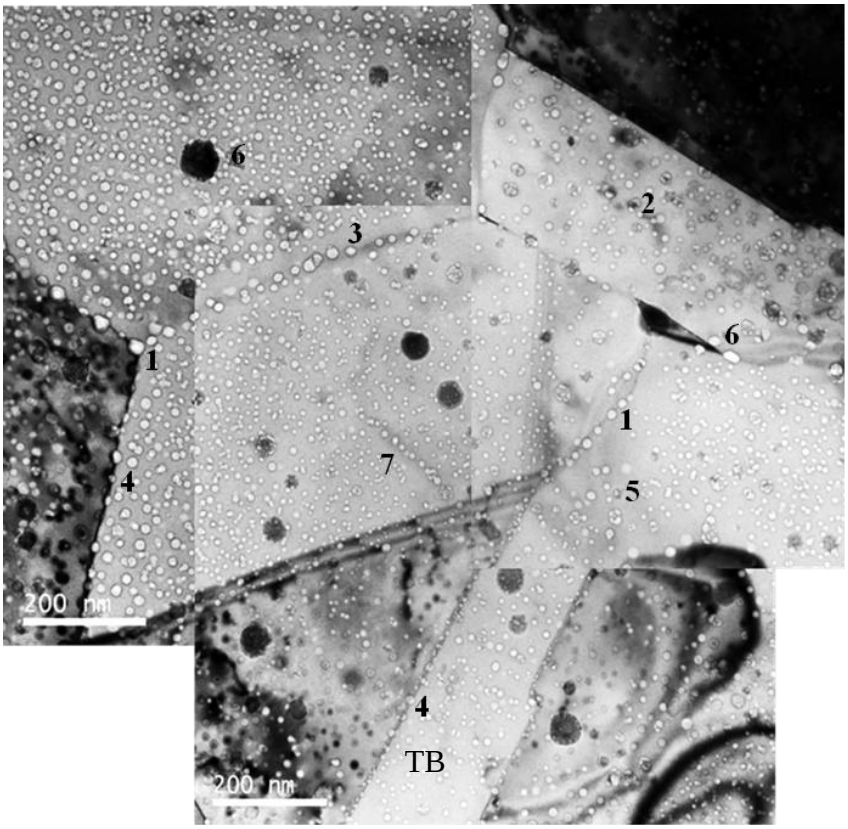

Fig. 5. Inhomogeneous distribution of inert gas bubbles in X18H10T-ODS steels. The numbers in the figure indicate the peculiarities of GP development in steel

A review of the literature revealed that the experimental data could be classified into three distinct categories: grains surrounded by fully denuded grain boundaries (FDZ), grains surrounded by at least half denuded grain boundaries (HDZ), and grains surrounded by no denuded grain boundaries (NDZ). Examples of such zones are shown in Fig. 5.

Grain boundaries or interfaces that have different crystallography or composition exhibit notably different structures and are therefore expected to demonstrate varying sink efficiencies. Consequently, the widths of zones denuded of vacancy clusters in close proximity to different types of GBs may differ, suggesting a degree of variation in GB sink/source efficiency [20–22].

Extensive research has been devoted to investigating the correlation between DZ formation and GB misorientation angle as well as grain size [23]. Results have revealed that both low-angle and high-angle boundaries can be denuded or non-denuded, and no discernible trend linking DZ formation and size with misorientation angle was observed. This suggests the presence of an additional parameter that impacts GB sink efficiency. Further research has demonstrated that these processes are reliant on other factors beyond misorientation angle, such as the GB plane [24]. Additionally, it has been demonstrated that DZ formation is influenced not only by misorientation angle, grain size, and GB type (high-angle or low-angle), but also by other factors.

The analysis also revealed a highly non-uniform distribution of gas bubbles throughout the grain volume. Large bubbles formed only near GBs, in narrow zones parallel to the boundaries. In contrast, small bubbles with nearly identical diameters and high densities were

present throughout the remainder of the internal grain volume, far from dislocations. Moreover, some coarsening of the bubbles also occurred near dislocations.

Fig. 5 illustrates that certain bubbles are aligned in chains (7) along previous dislocation lines, even though there are no current dislocations present along these chains. This observation indicates significant movement of dislocations during irradiation. It is possible that the bubbles collided with the dislocations and were subsequently trapped by them, forming chains. However, the dislocations then moved away, leaving the entire chain in its original position.

Fig. 5 also shows that a large number of bubbles were formed in the vicinity of the twin boundary (TB). The distribution of these voids is roughly uniform and there are no obvious DZs along the TB. This observation is consistent with previous investigations on irradiated Cu: defect agglomerates around the coherent twin boundary are similar as those in the interior of grains [24].

As can be seen from Fig. 5, the cavities are clustered in proximity to the precipitates. The cavities started to nucleate and grow at the interface between some oxide particles and the matrix, indicating that the oxide/matrix interface serves as a vacancy sink. The high concentration of vacancies and inert gas atoms contributes to the nucleation of cavities at the interface, which is in agreement with previous observations in ODS ferritic/martensitic steels [25] and ODS austenitic steels [26]. In this case, denuded zones of small size are observed.

CONCLUSIONS

The formation of denuded zones on GB in 18Cr10NiTi-ODS steel with the addition of Y_2O_3-ZrO_2 nano-oxides irradiated with energetic Ar-ions in the dose range of 40…110 dpa with simultaneously implanted argon to the levels of 0.08…7 at.% at temperatures of 550…650 ºC was investigated. The results obtained in this study are summarized below.

Round cavities with sizes of 1…8 nm were formed after irradiation. The cavity size distribution correlates with the calculated damage and argon deposition profiles: the higher the dose and argon concentration, the larger the cavities.

Denudation of grain boundaries is observed at depths beginning at 200 nm, where the argon concentration exceeds 0.4 at.% and the damage dose exceeds 50 dpa. DZ width ranges from 17 to 25 nm for the entire range of damage and the dose rate at the temperature of maximum swelling.

The cavity DZ width tends to increase with increasing irradiation temperature.

Argon cavities DZ were found to be smaller compared to the void DZ. This phenomenon is likely due to the formation of Ar-vacancy complexes with high migration energy.

The development of gas porosity and the formation of DZs in 18Cr10NiTi-ODS steel has a complicated character, which is attributed to its elevated GB population and the presence of nanosized oxide precipitates.

ACKNOWLEDGEMENTS

The work was financially supported by the National Academy of Science of Ukraine (program "Fundamental scientific research on the most important problems of the development of scientific and technical, socio-economic, socio-political, human potential to ensure Ukraine's competitiveness in the world and sustainable development of society and the state") and the European Federation of Academies of Sciences and Humanities (ALLEA), within the framework the "European Fund for Displaced Scientists", Grant EFDS-FL2-04.

REFERENCES

1. X.M. Bai, A.F. Voter, R.G. Hoagland, M. Nastasi, B.P. Uberuaga. Efficient Annealing of Radiation Damage Near Grain Boundaries via Interstitial Emission // *Science*. 2010, v. 327, p. 1631-1634.

2. M.J. Demkowicz, R.G. Hoagland, J.P. Hirth. Interface Structure and Radiation Damage Resistance in Cu-Nb Multilayer Nanocomposites // *Phys. Rev. Lett.* 2008, 100:136102.

3. T.D. Shen, S. Feng, M. Tang, J.A. Valdez, Y. Wang, K.E. Sickafus. Enhanced radiation tolerance in nanocrystalline $MgGa_2O_4$ // *Appl. Phys. Lett*. 2007, v. 90, p. 263115.

4. G.L. Kulcinski, B. Mastel, H.E. Kissinger. Characterization and annealing behavior of voids in neutron-irradiated nickel // *Acta Metall.* 1971, v. 19, p. 27-36.

5. A. Gentils, C. Cabet. Investigating radiation damage in nuclear energy materials using JANNuS multiple ion beams // *Nucl. Instrum. Methods.* 2019, v. B 447, p. 107-12.

6. G. Tolstolutskaya, S. Karpov, A. Kalchenko, I. Kopanets, A. Nikitin, V. Voyevodin. Effect of argon-ion irradiation on cavity formation and evolution in 18Cr10NiTi austenitic steel // *PAST*. 2020, N2(126), p. 27-32.

7. G. Tolstolutskaya, V. Ruzhytskyi, V. Voyevodin, I. Kopanets, S. Karpov, A. Nikitin. The role of radiation damage on retention and temperature intervals of helium and hydrogen detrapping in structural materials // *J. Nucl. Mater*. 2013, v. 442, p. S710-S714,

8. A.N. Velikodnyi, V.N. Voyevodin, A.S. Kalchenko, S.A. Karpov, I.V. Kolodiy, M.A. Tikhonovsky, G.D. Tolstolutskaya, F.A. Garner. Impact of nano-oxides and injected gas on swelling and hardening of 18Cr10NiTi stainless steel during ion irradiation // *J. Nucl. Mater.* 2022, v. 565, p. 153666.

9. A.N. Velikodnyi, V.N. Voyevodin, M.A. Tikhonovsky, V.V. Bryk, A.S. Kalchenko, S.V. Starostenko, I.V. Kolodiy, V.S. Okovit, A.M. Bovda, L.V. Onischenko, G.Y. Storogilov. Structure and properties of austenitic ODS steel 0818Cr10NiTi // *PAST.* 2014, N 1(92), p. 94-102.

10. G.D. Tolstolutskaya, V.V. Ruzhytskiy, I.E. Kopanetz, V.N. Voyevodin, A.V. Nikitin, S.A. Karpov, A.A. Makienko, T.M. Slusarenko. Accelerating complex for study of helium and hydrogen behavior in conditions of radiation defects generation // *PAST.* 2010, N 4(65), p. 135-140.

11. http://www.srim.org/
12. ASTM E521-96, 2009, ASTM.
13. I. Kolodiy, O. Kalchenko, S. Karpov, V. Voyevodin, M. Tikhonovsky, O. Velikodnyi, G. Tolmachova, R. Vasilenko, G. Tolstolutska. Microstructure and Hardening Behavior of Argon-Ion Irradiated Steels 18Cr10NiTi and 18Cr10NiTi-ODS // *East European Journal of Physics.* 2021, N 2, p. 105-114.
14. G.D. Tolstolutskaya, S.A. Karpov, A.S. Kalchenko, I.E. Kopanets, A.V. Nikitin, and V.N. Voyevodin. Effect of argon-ion irradiation on cavity formation and evolution in 18Cr10NiTi austenitic steel // *PAST. Series "Physics of Radiation Effect and Radiation Materials Science".* 2020, N 2, p. 27-32.
15. Y.-R. Lin, A. Bhattacharya, S.J. Zinkle. Analysis of position-dependent cavity parameters in irradiated metals to obtain insight on fundamental defect migration phenomena // *Materials & Design*. 2023, v. 226, p. 111668.
16. G.S. Was. *Fundamentals of radiation materials science: metals and alloys.* Berlin: "Springer Verlag", 2007.
17. P.J. Goodhew. Cavity growth mechanism maps // *Scripta Metallurgica*. 1984, v. 18(10), p. 1069-1073.
18. H. Ullmaier. The influence of helium on the bulk properties of fusion reactor structural materials // *Nucl. Fusion*. 1984, v. 24, N 8, p. 1039-1084.
19. P.J. Goodhew, S.K. Tyler. Helium Bubble Behaviour in B.C.C. Metals below $0.65T_m$ // *Proc. Roy. Soc. Lond. Math. Phys. Sci.* 1981, v. 377, p. 151-184.
20. P. Thorsen, J. Bilde-Sørensen, B.N. Singh. Influence of grain boundary structure on bubble formation behaviour in helium implanted copper // *Mater. Sci. Forum Trans Tech*. Publ. 1996, p. 445-448.
21. W. Kesternich. Helium trapping at dislocations, precipitates and grain boundaries // *Radiat. Eff*. 1983, v. 78, p. 261-273.
22. P. Lane, P. Goodhew. Helium bubble nucleation at grain boundaries // *Philos. Mag*. 1983, v. A 48(6), p. 965-986.
23. O. El-Atwani, J.E. Nathaniel, A.C. Leff, J.K. Baldwin, K. Hattar, M.L. Taheri. Evidence of a temperature transition for denuded zone formation in nanocrystalline Fe under He irradiation // *Materials Research Letters*. 2017, v. 5(3), p. 195-200.
24. W. Han, M. Demkowicz, E. Fu, Y. Wang, A. Misra. Effect of grain boundary character on sink efficiency // *Acta Materialia*. 2012, v. 60, p. 6341-6351.
25. K. Yutani, H. Kishimoto, R. Kasada, A. Kimura. Evaluation of Helium effects on swelling behavior of oxide dispersion strengthened ferritic steels under ion irradiation // *J. Nucl. Mater*. 2007, v. 367-370, part A, p. 423-427.
26. H. Oka, M. Watanabe, H. Kinoshita, T. Shibayama, N. Hashimoto, S. Ohnuki, S. Yamashita, S. Ohtsuka. In situ observation of damage structure in ODS austenitic steel during electron irradiation // *J. Nucl. Mater*. 2011, v. 417, issues 1-3, p. 279-282.

Article received 16.02.2023

ВПЛИВ ГРАНИЦІ ЗЕРНА НА ХАРАКТЕР УТВОРЕННЯ ПОРОЖНИН У СТАЛІ Х18Н10Т ДЗО, ЩО ОПРОМІНЕНА ІОНАМИ Ar^+ З ЕНЕРГІЄЮ 1,4 МеВ

Г.Д. Толстолуцька, С.О. Карпов, О.С. Кальченко, М.А. Тихоновський

Досліджено формування денудованих від порожнин зон поблизу меж зерен у сталі Х18Н10Т-ДЗО з додаванням нанооксидів Y_2O_3-ZrO_2, опроміненої високоенергетичними іонами Ar у діапазоні доз 40…110 зсувів на атом з одночасною імплантацією аргону до рівнів 0,08…7 ат.% при температурах 550…650 ºС. Трансмісійна електронна мікроскопія була використана для вивчення еволюції мікроструктури та ширини денудованих зон. Виявлено, що ширина денудованих зон залежить від умов опромінення, таких як доза опромінення, швидкість створення зсувів і температура. Вивчено вплив подрібнення зерна і нанорозмірних оксидних преципітатів на характеристики денудованих зон.